Ibn Al-Haitham Journal for Pure and Applied Sciences
Journal homepage: jih.uobaghdad.edu.iq
PISSN: 1609-4042, EISSN: 2521-3407
IHJPAS. 2025, 38 (1)

Adsorption Efficiency Investigation of Polyacrylonitrile for Methyl Green Dye from Aqueous Solution

Omar K. Najm[1*], Juman A. Naser[2]

[1,2]Department of Chemistry, College of Education for Pure Science (Ibn Al–Haitham), University of Baghdad, Baghdad, Iraq.
*Corresponding Author.

Received: 23 May 2023 Accepted: 6 August 2023 Published: 20 January 2025
doi.org/10.30526/38.1.3520

Abstract
Due to several environmental contaminants, the textile industry's wastewater disposal presents significant dangers, including to drinkable water. This study aims to synthesize polyacrylonitrile (PAN) and examine how well it adsorbs methyl green color from aqueous solution. The synthesis steps were performed after the PAN was characterized using various techniques, including FTIR, SEM, EDS, TGA-DSC, and XRD. Research was conducted on the quantity of adsorbent utilized, the initial concentration, and the contact time. All of these factors were shown to impact the adsorption process. The findings indicated that a dose of 0.01 g, an initial concentration of 30 mg/L, and a contact duration of 60 minutes produced the best results with the adsorbent. Using the Langmuir and Freundlich adsorption model, the maximum adsorption capacity was calculated to be 1604.837 mg/g. After applying Freundlich Langmuir and isotherm models to experimental adsorption data, the estimates made by the Freundlich model were more consistent with the experiments' actual results; thermodynamic analysis examined adsorption properties.
Keywords: Methyl green, polyacrylonitrile, adsorption, isotherm, maximum capacity.

1. Introduction

Due to the inclusion of several contaminants, such as acids, bases, toxins, organics, inorganics, dissolved solids, and color, the textile industry's wastewater disposal presents significant environmental dangers, including drinkable water. As a result, toxicological and aesthetic costs are associated with releasing pollutants like dyes into the environment since this practice degrades the quality of receiving streams and poisons creatures farther up the food chain. These colored chemicals reduce photosynthesis because they block sunlight in the stream and are thus visually unpleasant. With various organic dyes that are hazardous to people, color removal from processes and waste streams becomes ecologically significant (1).

Adsorption (2, 3), precipitation (4), physical-chemical methods (like filtration and distillation) (2, 4), and biological techniques, such as biosorption and phytoextraction (5, 6) are all examples of conventional procedures used to remediate polluted effluents.

Nevertheless, due to its low price, essential operation, uncomplicated construction, and the possibility of adsorbent recycling (7,8). Adsorption is now commonly employed. Studies have shown that materials, such as polymers, are gaining popularity for wastewater treatment to remove dye pollutants because they are inexpensive, abundant, and versatile in terms of their surface and structural qualities and their narrowly defined application area. Adsorption has eliminated several environmental toxins (9-12). Methyl green dye adsorption has been investigated by scientists (12,13) and their work on the surface of polyacrylonitrile (PAN) (14-16). This work used FTIR, SEM, EDS, and XRD to characterize PAN, an adsorbent that can remove methyl green from water. Adsorption was examined for several factors, including adsorbent dosage, initial concentration, and contact time. Using experiment data, Freundlich and Langmuir isotherm models calculated maximal capacity and adsorption energy. The thermodynamic analysis examined adsorption properties after using Freundlich Langmuir and isotherm models to analyze adsorption data. This study aims to synthesize PAN and discuss how well it adsorbs methyl green color from aqueous solutions.

2. Materials and Methods

2.1. Materials

Polyacrylonitrile $(CH_2CHCN)_n$, methyl green dye $C_{26}H_{33}N_3Cl_2$, dimethylformamide (DMF), distilled water, were the chemicals' sources. Sigma Aldrich was the source of all substances.

2.2. Instruments

Japanese Shimadzu spectrophotometer model S8400; Korean HYSC shaking water bath model SWB-25; Heater for the lab Hotplate stirrer (Model LMS-1003) from LabTech (Thailand) and a Daihan Labtech Oven (Model LDO-060E) from Germany. Intelligent mechanical HS-30D stirrer from Korea Scale with an electronic readout CPA-22/Sartorius/German. In other words, a scissor lift. Electron microscope (SEM) scan (S8000 TESCAN, French). Mechanically sliced. Thermal gravimetric TT-1000 analyzer (STA, Germany). The XRD-6000 spectrophotometer (Bruker, Germany) was used in conjunction with an atomic force microscope (Phywe, Germany) (Shimadzu, Japanese).

2.3. Polyacrylonitrile-based adsorbent

To prepare PAN with a W/V concentration of 25%, 5 g of PAN was dissolved in 20 mL of dimethylformamide solvent, heated to 30 °C on a hotplate stirrer until the solution became transparent and homogenous, dried in a thermal oven for hours at 70 °C until completely dry, then cut mechanically and screened by hand through a 600-um sieve.

2.4. Preparation of adsorbate

Methyl green, seen in **Figure 1.**, has the molecular formula $C_{26}H_{33}N_3Cl_2$, a molecular weight of 458.5 g/mol, and a maximum of 632 nm using a Double-Beam UV-Visible Shimadzu 1800 Spectrophotometer.

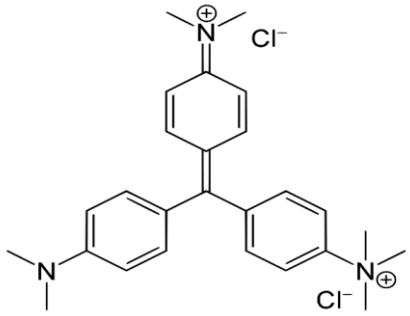

Figure 1. The chemical structure of methyl green dye.

A 0.25 g of methyl green dye was dissolved in 500 mL of distilled water to prepare the stock solution with a concentration (500 mg/L), from which the standard concentrations were obtained.

2.5. Adsorption experimental

The optimal amount of adsorbent for the methyl green dye adsorption process was studied (10 mL) at the initial concentration (25 mg/L) for 2 hours at 25°C. Polyacrylonitrile (0.01 g) is the perfect weight. The contact time was found by mixing 0.01 g of PAN with 10 mL of a 30 mg/L solution at 25 °C, ranging from 15 to 180 minutes.

The adsorption isotherm was investigated by dissolving 0.01 g of PAN in 10 mL of methyl green dye solution at 5, 10, 15, 20, 25, and 30 mg/L and having the mixture rest for 120 minutes at 25, 30, 35, and 40° C. Using a UV/V spectrometer, the absorbance of methyl green dye solution was measured at the maximum wavelength, and the quantity of adsorption was determined using the following equation:

$$q_e = \frac{(C_0 - C_e)V}{w} \quad (1)$$

C_0 is the dye starting concentration in milligrams per liter, C_e is the dye equilibrium concentration in milligrams per liter, V is the dye solution volume L, and W is the mass in grams.

3. Results and Discussion

3.1. Characterization

3.1.1. The FTIR technique

The PAN's infrared spectrum was captured between 600 and 4000 cm^{-1}, **Figure 2**. The chemical bonding and ionic radii pair CH_2, CN, C=O, C-O, and C-H are assigned several peaks. The C-H group stretching vibration in CH_2 and CH_3 was attributed to the 3024.37-2931.7 cm^{-1} absorption peak region (28). The nitrile group CN in PAN chains was ascribed to a distinctive absorption peak in the region 2245.13 cm^{-1}. Also, Absorption peaks of 1735.9 cm^{-1} and 1226.7 cm^{-1} indicated the presence of C=O and C-O groups, respectively, when PAN was exposed to air and the residual solvent. The resonance of the N-H bend was determined to cause the peaks at 1516.04 cm^{-1}. As a result, the stretching vibration of the C-H group explains the emergence of the peak at 1446.6 cm^{-1}. Aliphatic group C-H vibrations at various places in CH and CH_2 gave rise to absorption maxima at 1365.5 cm^{-1} and 1446.6 cm^{-1}, respectively (17,18).

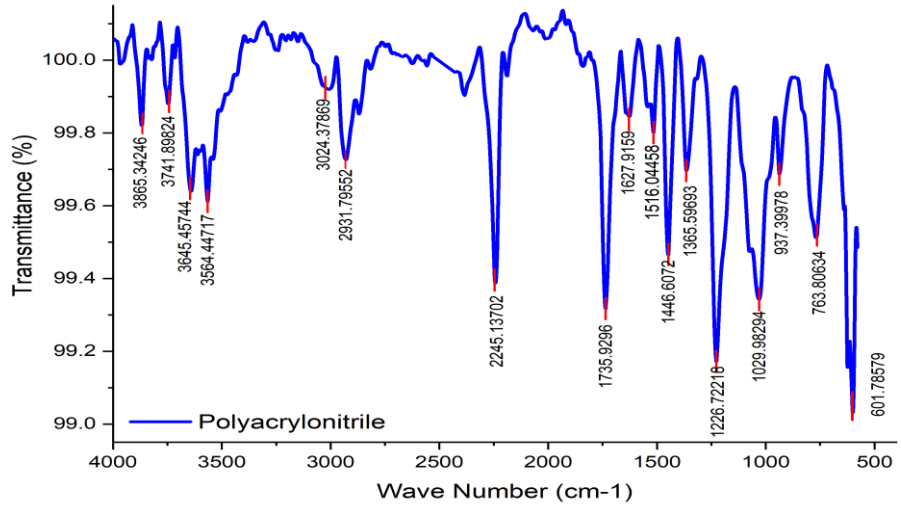

Figure 2. Infrared spectrum of the PAN.

3.1.2. The SEM technique

Figure 3. shows the surface morphology of the PAN created in these two photos, which shows that the basic polymer has been effectively manufactured. Each photograph shows individual strands of the polymer. When the two photos captured were examined at a magnification of 200 nm, the diameters of the fibers were not consistent; instead, they spanned a range from 31.26 nm to 57.41 nm (19).

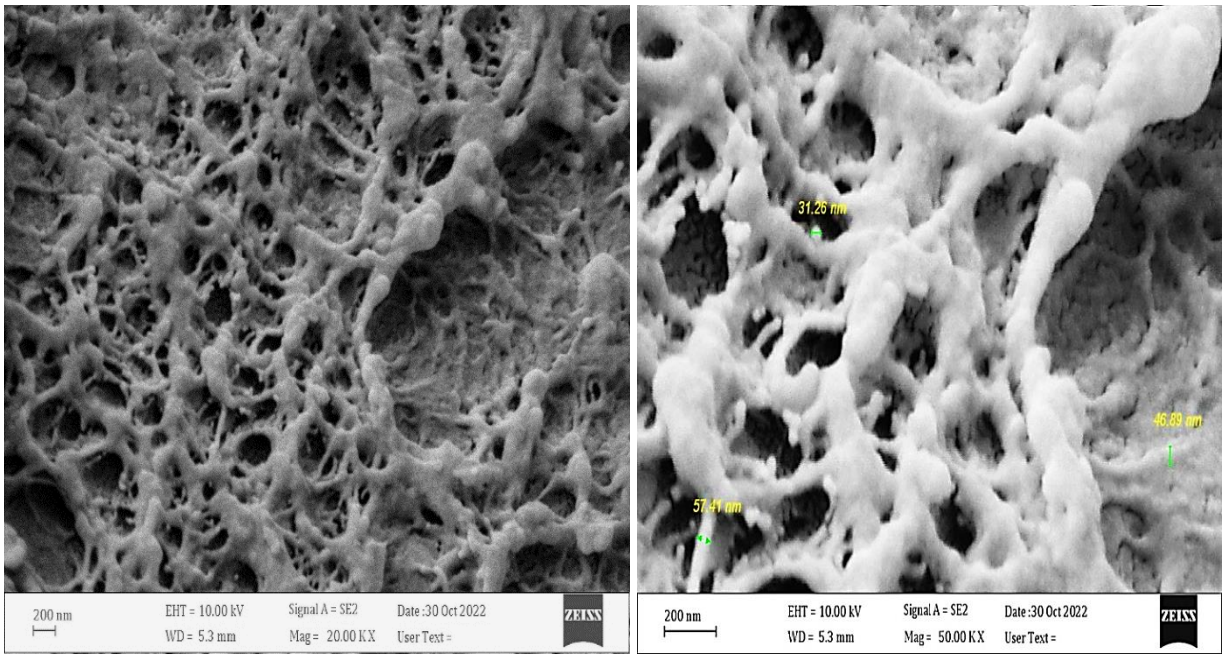

Figure 3. The SEM spectrum of the PAN.

3.1.3. The EDS technique

The EDS pattern on PAN is seen in **Figure 4.** Based on this distribution, we may deduce that the uppermost layer of the polymer solution is mainly made up of carbon and nitrogen (20). The carbon weight is 80.2, the nitrogen weight is 14.2, the oxygen weight is 3.9, and the iron

weight is 1.7. Some elemental oxygen was provided through polymer oxidation, while some was left over from the solvent. To get a good look at the insulating surfaces, we coat them with gold before we examine them. Coating describes this action. The elemental makeup, including the amount of each element, is detailed in **Figure 4**.

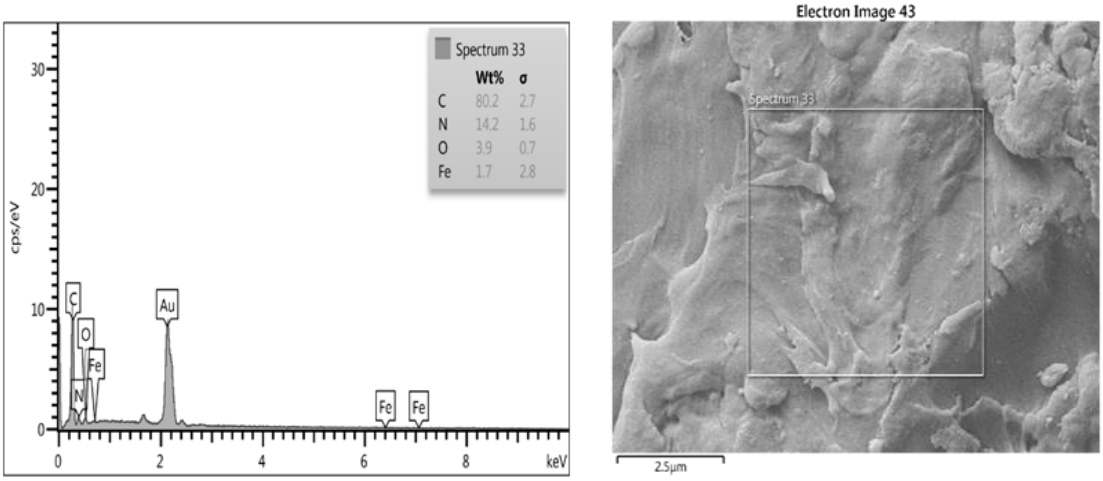

Figure 4. The EDS spectrum of PAN.

3.1.4. The XRD technique

The XRD diffraction pattern of PAN was obtained, as shown in **Figure 5.**, which indicates that the PAN retained the amorphous character. The XRD patterns have a central diffraction peak at around 2θ = 16.8° that belongs to level (022), which indicates the nature of the semi-crystalline structure of the polymer. So, the peak at the plane (101) has been returned to a hexagonal structure (related to C≡N) (21). Another weak peak was around 2θ= 25.5°, corresponding to ladder polymer (related to the C=N group). It fits the cyclization and aromatization structures of the 012, 023, 232, and 115 planes (22,23).

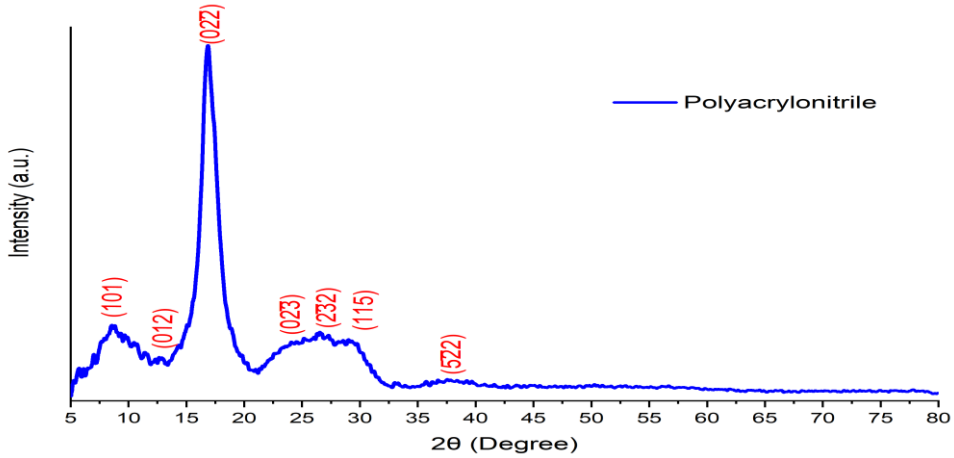

Figure 5. The XRD spectrum of PAN.

3.1.5. The TGA-DSC Technique

Thermogravimetric analysis (TGA) was used to probe the thermal degradation of PAN at 500°C at a rate of 10 degrees Celsius min-1 in an argon environment. PAN's two-stage thermal gram is depicted in **Figure 6**. Initial decomposition occurred between 100 and 250 °C, resulting in a loss of weight of 7.5 % due to evaporation, dehydration, or desorption of

water. The second stage, referring to the dissolution of the nitrile group, results in a weight loss of 83.5% at 300-403 °C. **Figure 6.** displays the DSC data, showing two distinct phases: an endothermic one at 316 °C and an exothermic one at 336 °C.

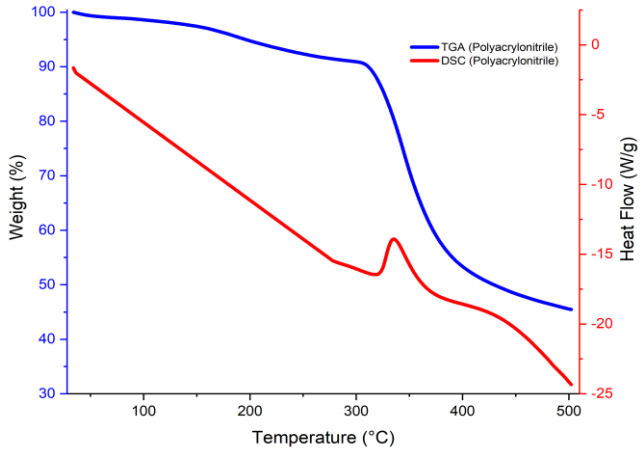

Figure 6. The TGA-DSC spectrum of PAN.

3.2. Optimization Study for the Adsorption Conditions

3.2.1. The Adsorbent Weight Effect

Figure 7. and **Table 1.** display the findings of a study conducted at 25 °C with an initial methyl green dye PAN concentration of 30 mg/L to determine the impact of adsorbent weight on adsorption. More PAN mass made more effective adsorption sites available, allowing more adsorptive dye. The optimal value was 0.01 g, which proved effective once the saturation stage was reached (24).

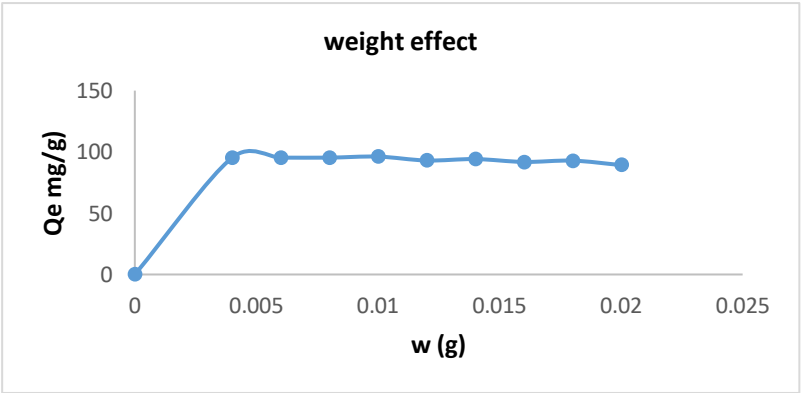

Figure 7. Adsorbent weight effect.

Table 1. The adsorbent weight effect.

Adsorbent	W (g)	Ads. %
PAN	0.0000	0.0000
	0.0040	95.2239
	0.0060	95.3290
	0.0080	95.3290
	0.0100	96.1783

	0.0120	92.9944
	0.0140	94.1613
	0.0160	91.8225
	0.0180	92.8874
	0.0200	89.2781

3.2.2. The Contact Time Effect

Figure 8. and **Table 2.** display the results of an experiment on the impact of contact time on the adsorption of methyl green dye onto PAN at 25 °C and an initial concentration of 30 mg/L. Adsorption linearly grows over time. Adsorption rates decrease significantly after 60 minutes (25-28) when equilibrium has been reached due to dye molecules occupying the most active spots on the surface of nanofibers.

Table 2. The contact time effect.

Adsorbent	T	Qe (mg/g)
PAN	0	0.0000
	15	26.2421
	30	20.5733
	45	20.9239
	60	20.2865
	75	21.0514
	90	21.2428
	105	28.1847
	120	26.7516

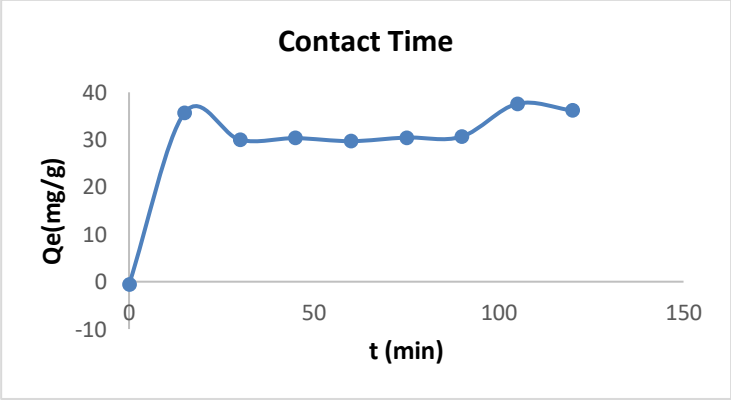

Figure 8. The contact time effect.

3.2.3. Adsorption isotherms

The adsorption isotherms show the equilibrium between the solution concentration and the quantity adsorbed on the adsorbent surface at a constant temperature. Since they describe the effectiveness between the adsorbent and the adsorbed species, adsorption isotherms may help you zero in on the optimal parameters for the adsorption process (26). In this experiment, it has been observed that methyl green dye adhered to PAN from its aqueous solution. The adsorption data have been modeled using the isotherms developed by Langmuir and Freundlich (**Figure 9.** and **Table 1.**). As the adsorption energy is uniformly distributed throughout the adsorbent surface, the Langmuir isotherm reveals that monolayer adsorption occurred at a single site. Here is how we might write Langmuir linearly (25,26).

$$\frac{C_e}{q_e} = \frac{1}{q_{max} k_L} + \frac{C_e}{q_{max}} \quad (2)$$

Where q_e is the equilibrium adsorbed concentration of dye in mg/g, C_e is the equilibrium adsorbed concentration of dye in mg/L, q_{max} is the maximum possible adsorbed concentration, and K_L is the experimental Langmuir constants. By examining the relationship between Ce/Qe and Ce, the values of the Langmuir constants were determined. The q_{max} is represented by the slope of the line, whereas the q_{max} is shown by the intercept.

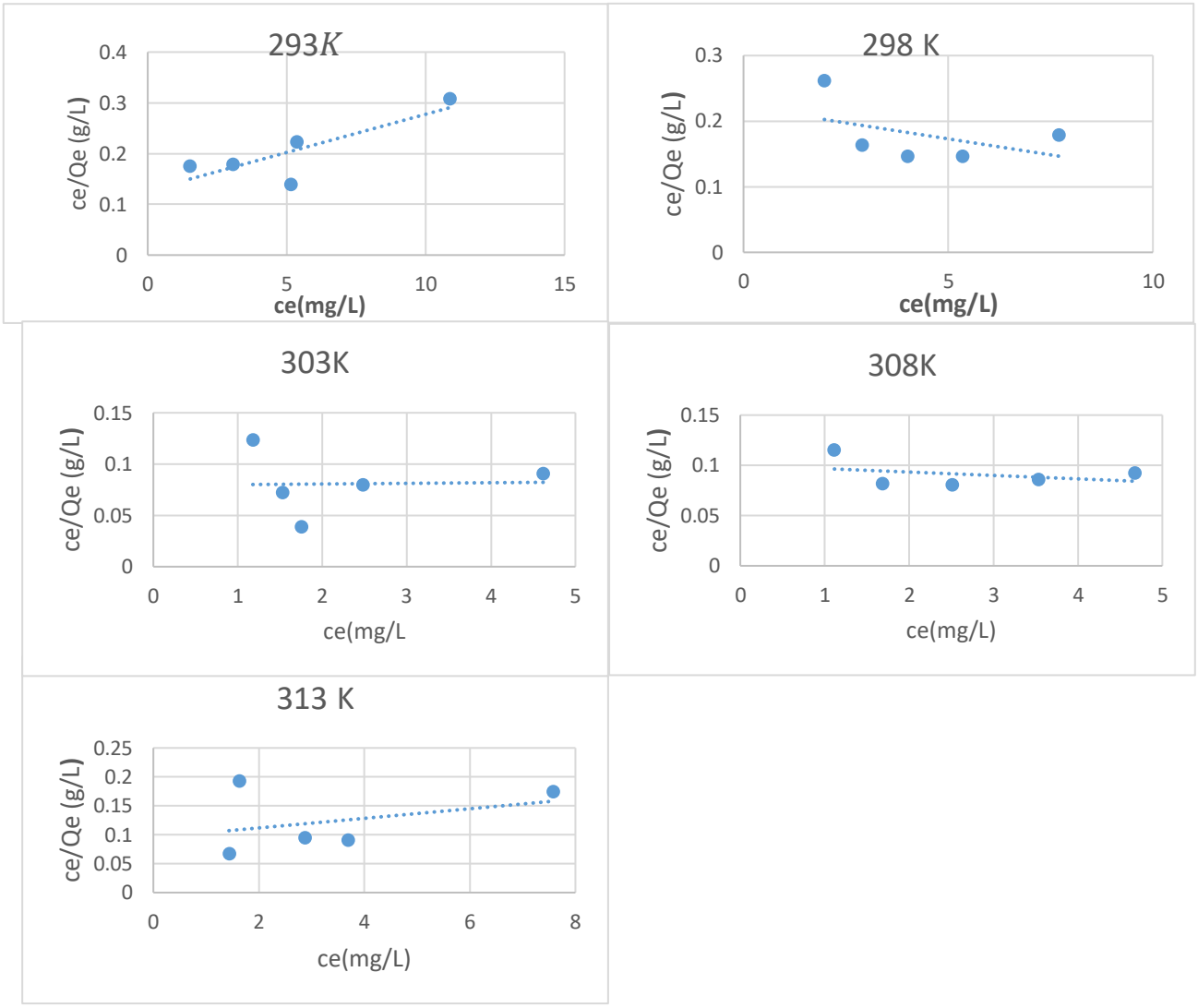

Figure 9. Langmuir isotherm plots of methyl green dye adsorption on PAN at the measured temperatures.

Table 1. Langmuir constants for the adsorption of methyl green dye onto PAN at the various temperatures considered.

Temperature (K)	R^2	Q_{max}	K_L
293	0.6714	66.4302	0.1186
297	0.2092	-102.5439	-0.0439
303	0.0008	1604.8366	0.0078
308	0.1187	-294.5489	-0.0339
313	0.1371	120.7369	0.0869

Table 2. shows that the KL and Qmax values fluctuated at various temperatures. In addition, the examined adsorption system has an average R2 value of 0.2274, indicating that the Langmuir model is inappropriate. It is assumed that the empirical equation known as the Freundlich isotherm model is applied to determine the energy distribution over a heterogeneous adsorbent surface **Figure 10**. Adsorption is only looked as if it is a multilayer (29,30). This is an expression for the linear Freundlich equation:

$$lnq_e = lnk_f + \frac{1}{n} lnC_e \quad (3)$$

Where q_e is the equilibrium adsorbed dye amount in mg/g, C_e is the equilibrium adsorbed dye concentration in mg/L, and k_f or n is the experimental Freundlich constant.

k_f and n can be calculated from the intercept and slope of plotting lnq_e versus lnC_e, respectively.

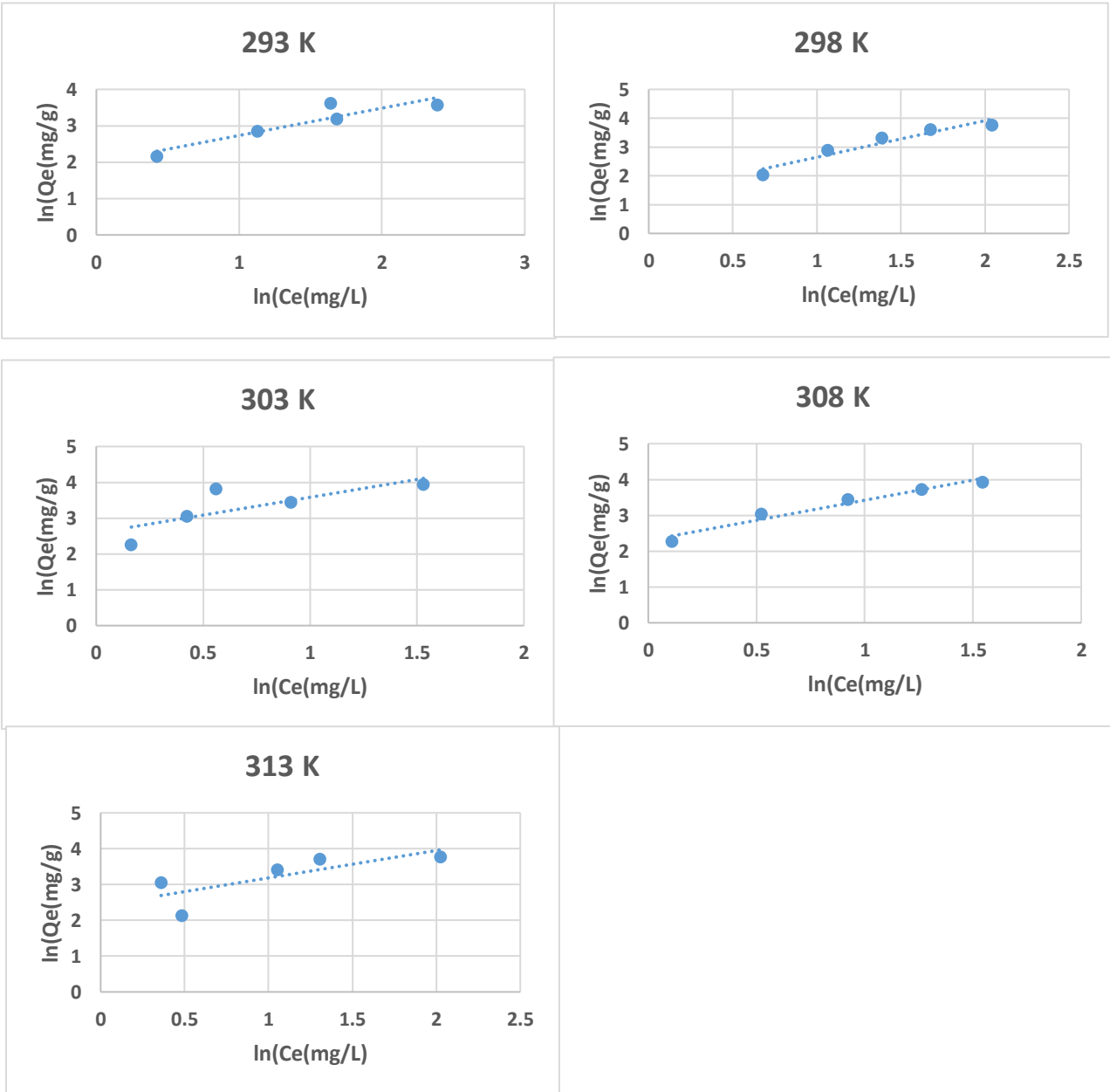

Figure 10. Freundlich isotherm plots of adsorption methyl green dye on PAN at the studied temperatures.

Table 2. Freundlich constants of adsorption of methyl green dye on PAN at the studied temperatures.

Temperature (K)	R^2	N	K_f
293	0.8394	1.3328	7.2665
297	0.9234	0.7875	3.9575
303	0.5996	1.0052	13.2879
308	0.9617	0.8926	9.9899
313	0.5943	1.3063	11.2173

The values of the Freundlich constant K_f, n were found to vary at the various temperatures under investigation, as shown in the table above. Consistently high values of R^2 indicate that the Freundlich model applies to the investigated adsorption process.

4. Conclusion

When the methyl green dye was extracted from an aqueous solution at various temperatures, the adsorbent properties of PAN performed admirably. It was discovered that the time required to reach equilibrium is 60 minutes and that 0.01 grams is the appropriate weight for the PAN surface employed for dye adsorption. Several analytical procedures were used to determine its properties, including FTIR, SEM, EDS, TGA-DSC, and XRD. Research was done on the variables that may affect how well adsorption occurred. The Freundlich and Langmuir constants for the adsorption system were computed, and it was determined that the Freundlich isotherm could use the results of those calculations.

Acknowledgment

The authors thank the Department of Chemistry at the College of Education for Pure Sciences (Ibn Al–Haitham) for conducting this study in its laboratories.

Conflict of Interest

The authors declare they have no competing interests.

Funding

There is no financial support.

Ethical Clearance

This work has been approved by the Scientific Committee at the University of Baghdad/ College of Education for Pure Science (Ibn Al-Haitham).

References

1. Karim AB, Mounir B, Hachkar M, Bakasse M, Yaacoubi A. Removal of basic red 46 dye from aqueous solution by adsorption onto Moroccan clay. J Hazard Mater. 2009; 168(1):304-309. https://doi.org/10.1016/j.jhazmat.2009.02.028
2. Souza C, Majuste D, Dantas MS, Ciminelli VS. Selective adsorption of gold over copper cyanocomplexes on activated carbon. Hydrometallurgy. 2014; 147(1):188-195. https://doi.org/10.1016/j.hydromet.2014.05.017

3. Haddou N, Ghezzar MR, Abdelmalek F, Ognier S, Martel M, Addou A. Plasmacatalytic removal of lead acetate assisted by precipitation. Chemosphere. 2014; 107(1):304-310. https://doi.org/10.1016/j.chemosphere.2013.12.071
4. Wang LY, Lee MS. Separation of Zr and Hf from sulfuric acid solutions with amine-based extractants by solvent extraction. Sep Purif Technol. 2015; 142(4):83-89. https://doi.org/10.1016/j.seppur.2015.01.001
5. Zulhairun AK, Ismail AF. The role of layered silicate loadings and their dispersion states on the gas separation performance of mixed matrix membrane. J Membr Sci. 2014;468(15):20-30. https://doi.org/10.1016/j.memsci.2014.05.038
6. Tabaraki R, Nateghi A, Ahmady-Asbchin S. Biosorption of lead (II) ions on Sargassum ilicifolium: application of response surface methodology. Int Biodeterior Biodegrad. 2014; 93(1):145-152. https://doi.org/10.1016/j.ibiod.2014.03.022
7. Yuan M, He H, Xiao L, Zhong T, Liu H, Li S, Deng P, Ye Z, Jing Y. Enhancement of Cd phytoextraction by two Amaranthus species with endophytic Rahnella sp. JN27. Chemosphere. 2014; 103(1):99-104. https://doi.org/10.1016/j.chemosphere.2013.11.040
8. Malana MA, Ijaz S, Ashiq MN. Removal of various dyes from aqueous media onto polymeric gels by adsorption process: their kinetics and thermodynamics. Desalination. 2010; 263(1-3):249-257. https://doi.org/10.1016/j.desal.2010.06.066
9. Ghati, S. K. Removal of Chlorpyrifos (Dursban) pesticide from aqueous solutions using barley husks. IHJPAS. 2017; 29(3):54-68.
10. Özavci S, Çetın B. Determination of radiation attenuation coefficients in concretes containing different wastes. Acta Physica Polonica A. 2016; 130(1):316-317. http://dx.doi.org/10.12693/APhysPolA.130.316
11. Akarslan F, Altinay Ö. Investigation on water retention properties of boric acid doped textile surfaces. Acta Physica Polonica A. 2015; 128(2B):405-406. http://dx.doi.org/10.12693/APhysPolA.128.B-405
12. Jawad H, Abbas AM. Study of efficacy adsorption of methyl green by attapulgite and modified attapulgite clay from aqueous solution. IHJPAS. 2021; 34(1):19-29. https://doi.org/10.30526/34.1.2550
13. Abbas AM, Abd SS, Himdan TA. Kinetic study of methyl green dye adsorption from aqueous solution by bauxite clay at different temperatures. IHJPAS. 2018; 31(1):58-66. https://doi.org/10.30526/31.1.1853
14. Jadoo SA, Naser JA. Adsorption thermodynamic study of Congo red dye on electrospun nanofibers mat of polyacrylonitrile. JGPT. 2019; 11(7):401-411. https://doi.org/10.1088/1757-899x/928/5/052024
15. Naser JA, Ahmed ZW, Ali EH. Nanomaterials usage as adsorbents for the pollutants removal from wastewater; A review. Materials Today: Proceedings. 2021; 42(1):2590-2595. https://doi.org/10.1016/j.matpr.2020.12.584
16. Naser JA, Himdan TA, Ibraheim AJ. Adsorption kinetic of malachite green dye from aqueous solutions by electrospun nanofiber Mat. Orient J Chem. 2017; 33(6):3121-3129. https://doi.org/10.13005/ojc/330654
17. Manocha LM, Bahl OP. Influence of carbon fiber type and weave pattern on the development of 2D carbon-carbon composites. Carbon. 1988; 26(1):13-21. https://doi.org/10.1016/0008-6223(88)90004-8
18. Fallahi D, Rafizadeh M, Mohammadi N, Vahidi B. Effect of LiCl and non-ionic surfactant on morphology of polystyrene electrospun nanofibers. e-Polymers. 2008; 18(056):1-10. https://doi.org/10.1515/epoly.2008.8.1.644

19. Jadoo SA, Naser JA. Adsorption optimization of congo red dye onto electrospun nanofibers of polyacrylonitrile functionalized with Fe_3O_4 nanoparticles. In IOP Conf Ser Mater Sci Eng. 2020; 928(052024):1-17. https://doi.org/10.1088/1757-899x/928/5/052024
20. Zhou W, Zhang Y, Du S, Chen X, Qi K, Wu T, Li J, Cui S, He J. Superwettable amidoximed polyacrylonitrile-based nanofibrous nonwovens for rapid and highly efficient separation of oil/water emulsions. ACS Appl Polym Mater. 2021; 3(6):3093-102. https://doi.org/10.1021/acsapm.1c00313
21. Al-heetimi DT, Dawood AH, Khalaf QZ, Himdan TA. Removal of methyl orange from aqueous solution by Iraqi bentonite adsorbent. IHJPAS. 2017; 25(2):328-339. Available from: https://doi.org/10.30526/25.2.1853
22. Al-Dulaimy ZA. Adsorption of bromo phenol red dye from aqueous solution by Iraqi bentonite clay. IHJPAS. 2017; 30(1):118-130. https://doi.org/10.30526/30.1.1065
23. Mahmood, OAA, Waisi BIS. Synthesis and characterization of polyacrylonitrile based precursor beads for the removal of the dye malachite green from its aqueous solutions. Desalin. Water Treat. 2021; 216:445-455. https://doi.org/10.5004/dwt.2021.26906
24. Fallahi, D, Rafizadeh, M, Mohammadi, N, Vahidi, B. Effect of applied voltage on jet electric current and flow rate in electrospinning of polyacrylonitrile solutions. Polymer international. 2008; 57(12):1363-1368. https://doi.org/10.1002/pi.2482
25. Ravi VP, Jasra RV, Bhat TS. Adsorption of phenol, cresol isomers and benzyl alcohol from aqueous solution on activated carbon at 278, 298 and 323 K. J Chem Technol Biotechno. 1998; 71(2):173-179.https://doi.org/10.1002/(SICI)1097-4660(199802)71:2%3C173::AID-JCTB818%3E3.0.CO;2-N
26. Mohammed AJ, Naser JA. Adsorption ability study of yellow (W6GS) dye from aqueous solution by Iraqi siliceous rocks. Poll Res. 2021; 40(1):58-62.
27. Saed UA. Batch and continuous adsorption of chromium (vi) from aqueous solution using alhagi forks and tea husk. Al-Nahrain J Eng Sci. 2016; 19(1):98-106. https://www.iasj.net/iasj/download/085d7427f4d825f1
28. Nasuha N, Hameed BH. Adsorption of methylene blue from aqueous solution onto NaOH-modified rejected tea. Chemical engineering journal. 2011; 166(2):783-786. https://doi.org/10.1016/j.cej.2010.11.012
29. Naser JA, Al-ani FA, Radhi IM, Himdan TA. Kinetic study of adsorption of malachite green dye on poly aniline-formaldehyde/chitosan composite. In IOP Conf Ser Mater Sci Eng. 2020; 928:052005. https://doi.org/0.1088/1757-899X/928/5/052005
30. Radhi, IM, Mohammed YI, Himdan TA, Badri DH. Adsorption of tetracycline on the bauxite and modified bauxite at different temperatures. IHJPAS. 2017; 30(3):150-157. https://doi.org/10.30526/30.3.1609